Journal of Molecular Catalysis A: Chemical 322 (2010) 39–44

Contents lists available at ScienceDirect

Journal of Molecular Catalysis A: Chemical

journal homepage: www.elsevier.com/locate/molcata

SO_2 reactivity on the MgO and CaO surfaces: A CW-EPR study of oxo-sulphur radical anions

Stefano Livraghi, M. Cristina Paganini*, Elio Giamello

Dipartimento di Chimica IFM, and NIS (Centre of Excellence), via Giuria 7, 10125 Torino, Italy

ARTICLE INFO

Article history:
Received 9 November 2009
Received in revised form 4 February 2010
Accepted 5 February 2010
Available online 13 February 2010

Keywords:
EPR
SO_2
Catalysis
Surface

ABSTRACT

Sulphur contamination of alkaline-earth oxide surfaces shows important consequences in many chemistry fields such as surface science and catalysis. We used the Electron Paramagnetic Resonance (EPR) technique to study the interaction of SO_2 molecules with the bare and electron enriched surfaces of MgO and CaO. Two paramagnetic products were identified via EPR thanks to this interaction, the $SO_2^{\bullet-}$ and $S_2O^{\bullet-}$ radicals whose abundance depends on the surface oxide properties. In particular, higher basicity and higher number of defects in the case of CaO lead to a higher amount of these two radical species.

1. Introduction

In our industrial society, sulphur oxides, mainly SO_2, are frequently produced as a result of burning sulphur-containing impurities present in coals and oil-derived fuels [1].

These impurities have a very negative impact on the processing of oil-derived chemical feedstock (catalyst poisoning, and equipment corrosion) and degrade the air quality in particular forming sulphur dioxide (SO_2). In the chemical and petrochemical industries millions of dollars are lost every year due to catalyst poisoning, and the negative effects of acid rain (main product of the oxidation of SO_2 in the atmosphere) on the environment and the corrosion of monuments or buildings are enormous. This toxic gas can cause severe irritation on the skin, eyes, mucous membranes, and respiratory system. There is a clear need to mitigate the negative effects of SO_2 [2,3].

Over the past 30 years several processes have been proposed and developed for the removal of SO_2 from various exhausts (deSOx operations). There is still no universally accepted solution to this problem. The implementation of new and more stringent regulations for the control of environmental pollution has encouraged the search for more efficient deSOx processes.

SO_2 adsorption on the surface of metal oxides [4], a key step in various deSOx reactions, is a rather complex process and has been the subject of several papers also in recent years [5–7]. Due to their basicity and high reactivity alkali earth oxides are particularly important in this field [8–11].

Alkali earth oxides can be useful as "throw-away" sorbents or can be combined with metals to generate catalysts for the reduction of sulphur dioxide to elemental sulphur.

It is well known that magnesium oxide and calcium oxide, especially in the presence of an oxidant promoter like CeO_2, show very high potential for SO_2 removal [9]. CaO based sorbents have been the leading materials for several decades in the field of deSOx [3,9,12], and magnesium oxide is a well-known sorbent in industrial processes. The interaction mechanism of these two basic oxides with sulphur oxides has not yet been fully elucidated. Several types of species are formed, in fact, depending on the surface hydroxylation degree and on the acid–base properties of the surface.

In principle, the SO_2 chemistry on a metal oxide can be very complex, because the molecule can either be adsorbed by a metal or interact with oxygen anions with formation of sulphites and sulphates groups [2,13,14]. S–O bond cleavage and full dissociation of the molecule can occur only on the metal centres. On metallic surfaces [15–18], the charge transfer between surface metal atom and SO_2 plays a dominant role in the binding and dissociation of SO_2. In general, such a similar charge transfer is difficult on oxide surfaces due to the low electron density on the metal cations [19–23].

Lunsford, years ago, demonstrated that sulphur dioxide reacts with MgO at room temperature to form sulphite and sulphate complexes [24–26]. At higher temperatures, infrared evidence suggests that sulphite ions react with molecular oxygen to form

* Corresponding author. Tel.: +39 011 6707576; fax: +39 011 6707855.
E-mail address: mariacristina.paganini@unito.it (M.C. Paganini).

1381-1169/$ – see front matter © 2010 Elsevier B.V. All rights reserved.
doi:10.1016/j.molcata.2010.02.012

bidentate sulphate complexes in addition to strongly bound SO_3. If trapped electrons are available on the surface of MgO, SO_2 also reacts to form the stable $SO_2^{\bullet-}$ ion [27]. To summarize, the chemistry of SO_2 on the surface of oxides is extremely complex and still obscure in many details. One possible way to rationalize this blurred picture consists in understanding correlations between chemical reactivity and particular properties of the solid.

The surface reactivity of SO_2, for instance, can be correlated with the basicity of the substrate [28,29,19]. In the sequence from MgO to BaO of alkaline-earth metal oxides (which all have the rocksalt structure) the lattice constant progressively and strongly increases, with parallel reduction of the Madelung field acting on the oxygen anions. As a consequence the electron-donor property (or the basicity) of the surface progressively increases with increasing the lattice parameter [30–32].

In the present paper we illustrate a study of SO_2 reactivity with MgO and CaO surface, by means of the Electron Paramagnetic Resonance. Both solids were used in two forms namely: (i) the bare, fully dehydroxylated, oxide and (ii) the so called "electron-rich" oxide containing surface trapped electrons [33–36].

The latter type of solid is known for its high electron transfer capability towards adsorbed molecules [23,37–41].

EPR is the reference technique to study electron transfer leading to molecules in paramagnetic state and its use to compare the reactivity of the two types of oxides is aimed at a better understanding of the surface chemistry of the oxides and, in particular, to discriminate between redox (electron transfer) and acid–base reactions (electron pair donation).

2. Experimental

High surface area MgO prepared by *Chemical Vapour Deposition* (*CVD*) was synthesized in the group of Prof. Diwald (T.U. Wien). Bare MgO was activated under vacuum (10^{-5} mbar at 1073 K for 1 h), to obtain a completely dehydrated material. The surface area of the activated oxide was 200 m^2/g. Similarly, bare CaO was obtained via slow thermal decomposition of commercial high-purity $CaCO_3$ (ex-Aldrich) under dynamic vacuum at 770 K for 16 h. The sample activation, to obtain a thoroughly dehydroxylated surface, was performed at 1173 K under a residual pressure of 10^{-5} mbar. The surface area of the resulting oxide is about 80 m^2/g. High-purity SO_2 was purchased by Aldrich and purified by the "freeze–thaw" method prior adsorption.

As anticipated in the previous section two distinct types of oxide materials were employed to study SO_2 adsorption on alkali earth oxides: the bare oxides and the corresponding electron-rich oxides. Briefly, the latter type of sample was prepared by irradiation of the activated solid with UV light under 100 mbar hydrogen at 77 K using a low pressure mercury vapour lamp. After 45 min irradiation the excess H_2 was slowly evacuated at 298 K. The electron-rich oxides are coloured in blue.

X-band CW-EPR spectra were recorded between 298 K and 77 K on a Bruker EMX spectrometer equipped with a cylindrical cavity operating a 100 kHz field modulation. The EPR computer simulations were obtained using SIM32S program developed by Prof. Sojka (Jagellonian University, Cracow Poland [42]), while double integration of the spectra was produced with the program Win-EPR. Traces of Mn^{2+} ions in the bulk of CaO are practically unavoidable and generate a weak EPR signal with the typical manganese sextet centred nearby the free electron *g* value. This signal always appears in the EPR spectra of CaO and has been used as internal standard for *g* values evaluation.

3. Results and discussion

3.1. EPR spectra after SO_2 adsorption

The surface reactivity of bare alkali earth oxides is dominated by the basicity associated to the O^{2-} ions which increases from MgO to CaO [33,43].

In the electron-rich surface (which contains very reactive $(H^+)(e^-)$ pairs) the basic reactivity does not vanish but is accompanied by the typical electron transfer reactivity associated to trapped electrons [40,41,44–47]. The two bare oxides are completely EPR silent with the exception of the weak sextet in CaO due to traces of bulk Mn^{2+} ions. As opposite, the two electron-rich oxides (hereafter MgO/$(H^+)(e^-)$ and CaO/$(H^+)(e^-)$) exhibit the typical EPR signal of surface trapped electrons close to the free electron resonance region which has been thoroughly described in a series of previous papers [33]. The EPR signal due to surface trapped electrons is characterized by a hyperfine doublet due to a weak residual interaction of the electron centre with the nearby proton.

Fig. 1 reports the EPR spectra obtained upon SO_2 contact with the three oxide samples. In the case of bare MgO the interaction with SO_2 does not produce any signal while intense signals are observed in the case of bare CaO (Fig. 1c) and electron-rich MgO (Fig. 1a) and CaO (Fig. 1b). In the two latter cases the new spectrum onset is accompanied by the total (MgO) or partial (CaO) disappearance of the trapped electrons signal.

Spectrum 1c, recorded for bare CaO, is due, as it will be detailed in the next section, to $SO_2^{\bullet-}$ radical ions adsorbed on the surface. In the two spectra related to electron-rich materials (1a and 1b) a second species, namely as $S_2O^{\bullet-}$ radical ion, is present beside $SO_2^{\bullet-}$ as documented by the low field feature at around $g = 2.030$ which is the finger print of $S_2O^{\bullet-}$ [24].

This second species becomes more evident at low temperature and, since it shows a different saturation behaviour with respect to $SO_2^{\bullet-}$, becomes predominant at high microwave power as shown in Fig. 2 where the spectra recorded at RT from 0.01 mW to 20 mW for SO_2 on CaO/$(H^+)(e^-)$ are reported. Fig. 2 insert shows the saturation plot for $S_2O^{\bullet-}$ which is linear (no saturation) in the whole range explored.

Another relevant difference in the reactivity between the two electron-rich oxides is the abundance of the $SO_2^{\bullet-}$ species generated by the interaction with the starting $(H^+)(e^-)$ centres. On

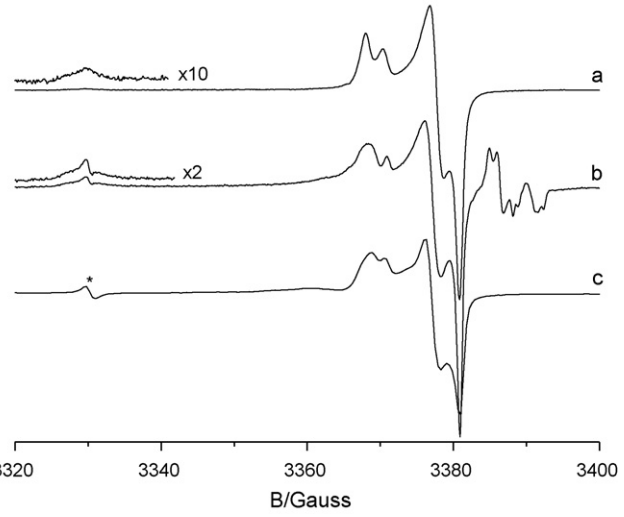

Fig. 1. EPR spectra of SO_2 adsorbed on: (a) MgO/$(H^+)(e^-)$, (b) CaO/$(H^+)(e^-)$ and (c) bare CaO. No EPR signal was detected on bare MgO. Star indicates Mn^{2+} lines. Spectra recorded at RT and 1 mW of microwave power.

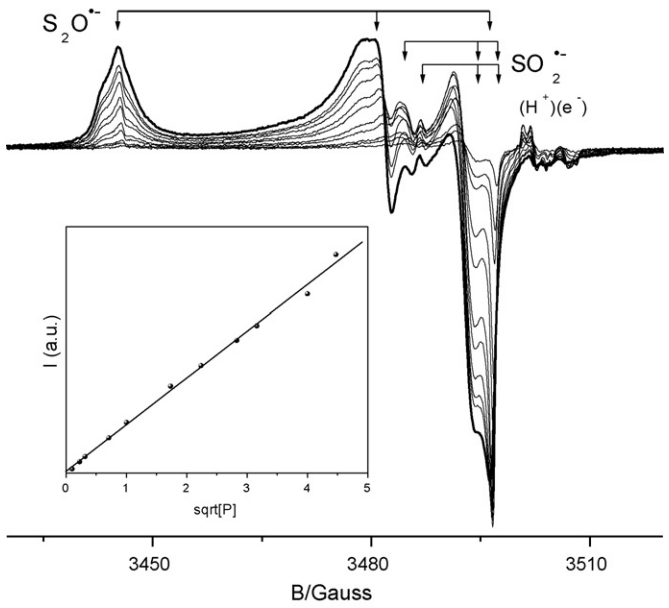

Fig. 2. EPR spectra of SO_2 on CaO/$(H^+)(e^-)$ at RT. Spectra recorded at variable microwave power from 0.01 mW to 20 mW. The insert reports the saturation plot obtained by double integration of the lower field component ($g = 2.030$) of the $S_2O^{\bullet-}$ signal.

$MgO(H^+)(e^-)$ (Fig. 1a) after 15 mbar gas adsorption the amount of $SO_2^{\bullet-}$ is roughly equivalent to that of the electrons trapped on the surface before adsorption whereas in the case of electron-rich CaO, $(H^+)(e^-)$ centres are still observable also after income of a higher amount (30 mbar) of SO_2 (Fig. 3). The sulphur concentration is, for electron-rich CaO, less than twice than the starting $(H^+)(e^-)$ signal (Table 1). Fig. 3 insert reports a magnification of the low field region of the spectrum which shows how the $S_2O^{\bullet-}$ species is formed in substantial amount only upon absorption at high pressure (30 mbar). This fact together with the results obtained for bare CaO (SO_2^- is formed – Fig. 1c – by direct contact with the clean surface in absence of trapped electrons) clearly indicates that in the

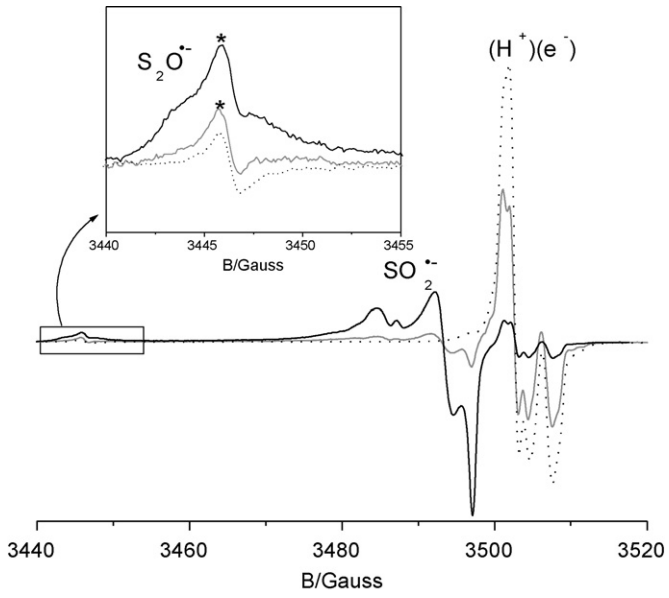

Fig. 3. Adsorption of SO_2 on CaO/$(H^+)(e^-)$. Dotted line: starting material. Grey line: adsorption of SO_2 (15 mbar). Black line: adsorption of SO_2 (30 mbar). The * symbol indicates Mn^{2+} impurity.

Table 1
EPR intensity (arbitrary units) obtained by double integration of EPR spectra in Fig. 1.

	Starting materials	SO_2 adsorption
MgO	–	–
$MgO(H^+)(e^-)$	1.0	0.95
CaO	–	0.31
$CaO(H^+)(e^-)$	1.0	1.42

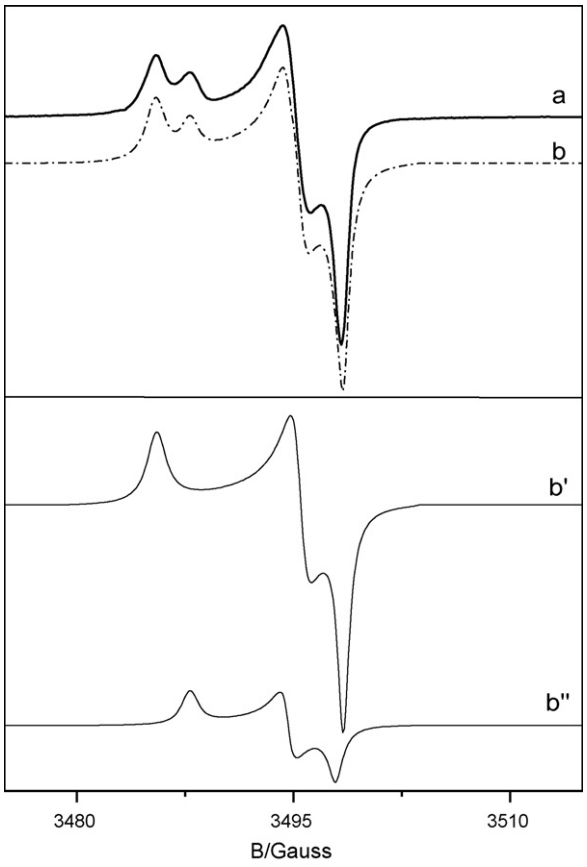

Fig. 4. Experimental (a) and simulated (b) EPR spectra of $SO_2^{\bullet-}$ species on $MgO(H^+)(e^-)$. Signals b^I and b^{II} are the individual signals employed in the simulation.

case of this oxide, SO_2 does not simply react with $(H^+)(e^-)$ centres only but undergoes a more complex reactivity.

3.2. Simulation of experimental spectra

The $SO_2^{\bullet-}$ radical anion has been observed in the past on different surfaces. In the case of MgO the presence of two slightly different species, whose abundance strictly depends on oxide surface pre-treatment, was reported [25]. In the present work SO_2 adsorption leads to $SO_2^{\bullet-}$ radical stabilization in all samples examined except for bare MgO.

In Fig. 4 the experimental trace (a) and the related simulation (b) due to SO_2 adsorption on MgO/$(H^+)(e^-)$ (also in Fig. 1c) are reported. The parameters employed are listed in Table 2. The $S_2O^{\bullet-}$ species was not introduced in this simulation as present in very low

Table 2
EPR parameters for the simulation of $SO_2^{\bullet-}$ species observed after SO_2 adsorption on MgO/$(H^+)(e^-)$.

Species	Abundance %	$g_1-\Delta H_1$ (G)	$g_2-\Delta H_2$ (G)	$g_3-\Delta H_3$ (G)
$SO_2^{\bullet-}$ (b^I)	78	2.008–0.6	2.003–0.9	2.001–1
$SO_2^{\bullet-}$ (b^{II})	22	2.007–0.9	2.003–0.6	2.001–0.6

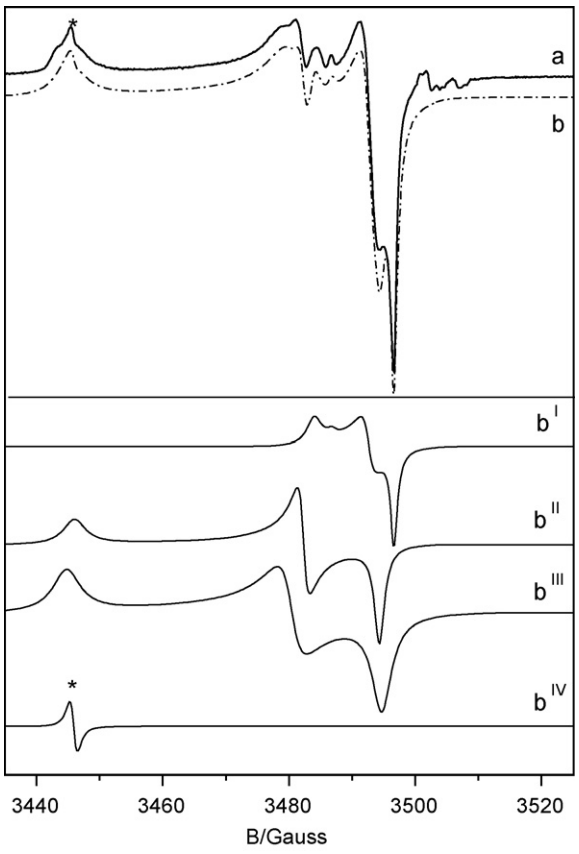

Fig. 5. Experimental (a) and simulated (b) EPR spectra of the species observed after SO_2 adsorption on CaO/$(H^+)(e^-)$. Experimental spectrum recorded at RT and 8 mW. Signals b^I, b^{II} and b^{III} are the individual traces related to $SO_2^{\bullet-}$ (b^I) and $S_2O^{\bullet-}$ (b^{II} and b^{III}) species while b^{IV} is due to Mn^{2+}. For the sake of simplicity residual $(H^+)(e^-)$ centres were not simulated.

concentration. The spectrum is composed by the superimposition of two signals with a quasi axial *g* tensor and has the structure expected for 19 electrons three-atomic radicals like $O_3^{\bullet-}$ or $ClO_2^{\bullet}$ whose *g* tensor is only slightly affected by the surrounding crystal field [24]. Fig. 5 reports the spectrum experimental trace (a) and the simulation (b) observed after SO_2 adsorption on CaO/$(H^+)(e^-)$ and recorded at 8 mW microwave power. The spectrum is quite complex due to the superimposition of several distinct signals individually reported in the second part of Fig. 5 (lines from b^I to b^{IV}). The simulation in Fig. 5b (see also Table 3) has been obtained considering (apart the Mn^{2+} impurity, b^{IV}) the presence of both $SO_2^{\bullet-}$ (two similar species like in the previous case both included in line b^I) and $S_2O^{\bullet-}$ (two similar species, b^{II} and b^{III}). The $S_2O^{\bullet-}$ species has been already observed in the past. In particular Lunsford and co-workers reported the same radical species, generated by co-adsorption of H_2S and SO_2 [27] on the surface of MgO. As in the case of $SO_2^{\bullet-}$, this is a 9 electrons radical species, its *g* tensor is not much affected by the surrounding crystal field. For this reason the spectral features here observed do not sensibly change moving from CaO to MgO.

3.3. Reaction mechanisms

The SO_2 interaction with alkali earth oxides was largely studied in the past with various techniques for its importance in heterogeneous catalysis. It is well established that various types of reaction channels exist including those involving diamagnetic species. In particular SO_2 interaction with low coordinated surface oxygen (O_{LC}^{2-}) leads to diamagnetic surface species [48,49], the main one being SO_3^{2-} formed according to

$$SO_2 + O_{LC}^{2-} \rightarrow SO_3^{2-} \quad (1)$$

In particular conditions surface sulphates (SO_4^{2-}) and elemental sulphur have been observed also.

In the present paper we explored paramagnetic channels which, as expected, take place on electron-rich surfaces but also, in the case of CaO, on bare surfaces. We have basically shown that:

(a) On the surface containing reducing centres $(H^+)(e^-)$ the direct electron transfer to SO_2 with $SO_2^{\bullet-}$ formation easily occurs

$$SO_2 + (H^+)(e^-) \rightarrow SO_2^{\bullet-} + (H^+)(-) \quad (2)$$

However the two-sulphur $S_2O^{\bullet-}$ species is also formed in the same process indicating a reactions complexity well beyond the direct electron transfer. This consideration applies in particular to the case of the electron-rich CaO ($S_2O^{\bullet-}$ in this case represents one third of the total radical production) while in the case of MgO the amount of $S_2O^{\bullet-}$ formed is very low and the concentration of $SO_2^{\bullet-}$ roughly corresponds to that of trapped electrons.

(b) While bare MgO does not produce paramagnetic entities upon contact with SO_2, the more basic calcium oxide origins $SO_2^{\bullet-}$ surface radical ions even in the absence of surface trapped electrons.

Such a difference between the behaviour of two oxide has been already observed in the past, and the propensity of these two oxides to stabilize different radical species in the case of the same adsorbed molecule has been well documented, in several paper concerning O_2 and NO interaction [37,50,51].

The formation of $SO_2^{\bullet-}$ on bare CaO is understood in terms of a disproportionation reaction induced by basic O_{LC}^{2} sites. Similar reactions, for instance, have been observed for CO on basic oxide [52] which is reduced to carbon oxoanions (oxidation number lower than 2) and simultaneously oxidized to surface carbonates (ON = 4) by interacting with surface basic sites.

$SO_2^{\bullet-}$ formation mechanism (Eq. (3)) can be thus written as follows:

$$3SO_2 + 2O_{LC}^{2-} \rightarrow 2SO_2^{\bullet-} + SO_4^{2-} \quad (3)$$

Table 3
EPR parameters (abundance, *g* value and line-width) of the various species observed after SO_2 adsorption on CaO/$(H^+)(e^-)$. In the lower part some literature data for different sulphur radicals on MgO are reported.

Species	Abundance %	g_1–ΔH_1 (G)	g_2–ΔH_2 (G)	g_3–ΔH_3 (G)	Ref.
(b^I) $SO_2^{\bullet-}$	61	2.008–1.7	2.003–1.6	2.001–0.7	This work
(b^{II}) $SO_2^{\bullet-}$	5	2.007–0.9	2.003–1.0	2.001–1.0	
(b^{III}) $S_2O^{\bullet-}$	20.8	2.030–2.5	2.009–1.2	2.003–1.1	
(b^{IV}) $S_2O^{\bullet-}$	12.4	2.031–3.1	2.011–2.7	2.002–2.2	
(A) $SO_2^{\bullet-}$/MgO	–	2.010	2.005	2.003	[25]
(B) $SO_2^{\bullet-}$/MgO	–	2.008	2.003	2.001	[25]
$S_2O^{\bullet-}$/MgO	–	2.030	2.010	2.001	[24]

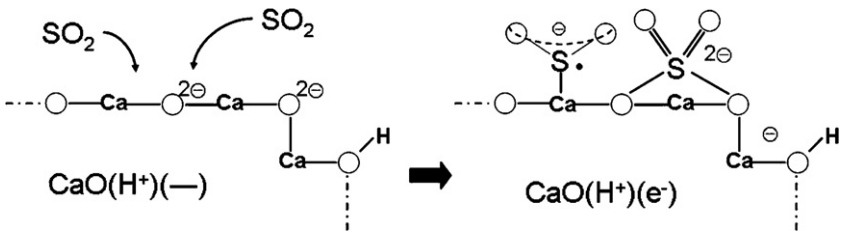

Scheme 1. Sketch representing reactions (4)–(6) for the SO_2 adsorption at the partially hydrogenated CaO surface.

This mechanism can be decomposed in two sub-reactions where released electrons (Eq. (4)) can react with SO_2 in the same way of $(H^+)(e^-)$ centres forming the paramagnetic $SO_2^{\bullet-}$ species (Eq. (5)).

$$SO_2 + 2O_{LC}^{2-} \rightarrow SO_4^{2-} + 2e^- \quad (4)$$

$$SO_2 + e^- \rightarrow SO_2^{\bullet-} \quad (5)$$

The overall reaction (3) should be enough to fully explain the $SO_2^{\bullet-}$ generation on bare CaO but sub-reaction (4) is unable to explain the presence of unexpected $(H^+)(e^-)$ centres in the case of the $CaO(H^+)(e^-)$ system (Fig. 3). It is well established [33] that $(H^+)(e^-)$ centres are high reactive species but, when reaction (4) occurs in proximity of the bleached colour centre $[(H^+)(—)]$ a fraction of the released electrons, can be trapped again (Scheme 1) regenerating the surface colour centres (Fig. 3) according to:

$$(H^+)(—) + e^- \rightarrow (H^+)(e^-) \quad (6)$$

This last reaction, in the case of bare CaO, cannot take place because of the absence of surface hydroxyl groups. Electrons in fact need the presence of neighbouring OH groups to be stabilized at the alkali earth oxide surfaces. While $SO_2^{\bullet-}$ formation mechanism, described above, is supported by robust pieces of evidence, the formation of $S_2O^{\bullet-}$ (which occurs abundantly on electron-rich CaO) is not clear in all details. The mechanism illustrated in the following remains therefore partially tentative.

Also in this case the CaO surface and in particular the presence of surface defects play a crucial role and we cannot exclude the presence of parallel reaction mechanisms leading to the same products. To find out a $S_2O^{\bullet-}$ formation consistent mechanism we move from a Rodriguez et al. [2] finding who showed that after SO_2 adsorption on MgO(1 0 0) films at 300 K an extensive dissociation of the molecule occurs ($SO_2 \rightarrow S_{ads} + 2O_{ads}$). On the basis of this and other results the authors suggest that Mg atoms with a low coordination (<5) may be able to dissociate SO_2. This idea was confirmed working with a defective MgO_{1-x} system prepared by soft sputtering of MgO(1 0 0) films with Ar^+ ions. This procedure preferentially removes O atoms from oxide surfaces and the authors showed, for the adsorption of SO_2 on this MgO_{1-x} system, SO_4^{2-}, SO_3^{2-}, and S coexistence on the oxide substrate. All these experiments were carried out on magnesium oxide only, but the conclusion can be easily extended to the CaO system since, it is well known that this oxide has the same structure and a higher reactivity than MgO. The same dissociation effect likely occurs also on the oxides used in the present work because they are prepared in high surface area form and therefore contain a high surface defects number corresponding to low coordination ions [51]. If sulphur atoms are present at the oxide surface the following reaction could easily occurs

$$2SO_2 + S \rightarrow S_2O + SO_3 \quad (8)$$

forming a reduced (S_2O) and an oxidized (SO_3) sulphur oxide. The latter easily reacts on the surface forming sulphates ions:

$$SO_3 + O_{LC}^{2-} \rightarrow SO_4^{2-} \quad (9)$$

Independently from the generation mechanism, the diamagnetic S_2O species must be present on the surface. In fact S_2O further reacts with trapped electrons to form the paramagnetic $S_2O^{\bullet-}$ species (reaction (10)).

$$S_2O + (H^+)(e^-) \rightarrow S_2O^{\bullet-} + (H^+)(—) \quad (10)$$

The last step (10) is in full agreement with the fact that $S_2O^{\bullet-}$ formation occurs only on the systems containing surface trapped electrons. On bare CaO and MgO this species, in fact, was not observed. The higher $S_2O^{\bullet-}$ amount formed on $CaO(H^+)(e^-)$ with respect to $MgO(H^+)(e^-)$ is likely due to the higher CaO reactivity leading to an abundant formation of the S_2O precursor (8).

4. Conclusion

SO_2 is known to react with the surface of basic oxides following different reaction channels. We have described and followed by EPR those channels involving paramagnetic species. The two oxides' reactivity with SO_2, both in bare and in electron-rich forms ($CaO(H^+)(e^-)$, $MgO(H^+)(e^-)$), has been monitored and two distinct radical anions' ($SO_2^{\bullet-}$ and $S_2O^{\bullet-}$) formation has been put in evidence.

The $SO_2^{\bullet-}$ formation mechanisms are explicitly described (direct electron transfer or surface disproportionation) while the mechanism of $S_2O^{\bullet-}$ (which forms an electron-rich surface only) was been tentatively proposed.

References

[1] J.A. Rodriguez, T. Jirsak, M. Perez, S. Chaturvedi, M. Kuhn, L. Gonzalez, A. Maiti, J. Am. Chem. Soc. 122 (2000) 12362–12370.
[2] J.A. Rodriguez, T. Jirsak, A. Freitag, J.Z. Larese, A. Maiti, J. Phys. Chem. B 104 (2000) 7439–7448.
[3] Z. Xingying, Z. Guoshun, C. Jianmin, W. Ying, W. Xiao, A. Zhisheng, Z. Peng, J. Phys. Chem. B 110 (2006) 12588–12596.
[4] M. Waqif, A.M. Saad, M. Bensitel, J. Bachelier, O. Saur, J. Lavalley, J. Chem. Soc., Faraday Trans. 88 (1992) 2931–2936.
[5] J.A. Rodriguez, Catal. Today 85 (2003) 177–192.
[6] I. Hong, H. Jiang, Y.D. Park, J.Y. Kim, B.H. Ha, Chem. Phys. Lett. 366 (2002) 572–577.
[7] J.A. Rodriguez, J. García, L. González, Chem. Phys. Lett. 365 (2002) 380–386.
[8] R. De Francesco, M. Stener, G. Fronzoni, J. Phys. Chem. C 111 (2007) 13554–13563.
[9] E. Sasmaz, J. Wilcox, J. Phys. Chem. C 112 (2008) 16484–16490.
[10] Y. Shi, H. Pan, Y. Zhang, W. Li, Catal. Commun. 9 (2008) 796–800.
[11] L. Oliviero, H. Leclerc, O.V. Manoilova, V. Blasin-Aube, F. Mauge, E.V. Kondratieva, M.S. Poretsky, A.A. Tsyganenko, Ind. Eng. Chem. Res. 44 (2009) 1237–1241.
[12] L.S. Jae, H.K. Jun, S.Y. Jung, T.J. Lee, C.K. Ryu, J.C. Kim, Ind. Eng. Chem. Res. 44 (2005) 9973–9978.
[13] A. Pieplu, O. Saur, J.C. Lavalley, O. Legendre, C. Nedez, Catal. Rev. Sci. Eng. 40 (1998) 409–450.
[14] V.E. Henrich, P.A. Cox, The Surface Science of Metal Oxides, Cambridge University Press, Cambridge, 1994.
[15] J.A. Rodriguez, J.M. Ricart, A. Clotet, F. Illas, J. Chem. Phys. 115 (2001) 454–465.
[16] S. Sakaki, H. Sato, Y. Imai, K. Morokuma, K. Ohkubo, Inorg. Chem. 24 (1985) 4358–4544.
[17] H. Sellers, E. Shustorovich, Surf. Sci. 346 (1996) 322–336.
[18] J.A. Rodriguez, T. Jirsak, S. Chaturvedi, J. Hrbek, J. Am. Chem. Soc. 120 (1998) 11149–11157.
[19] G. Pacchioni, A. Clotet, J.M. Ricart, Surf. Sci. 315 (1994) 337–350.
[20] G. Pacchioni, J.M. Ricart, F. Illas, J. Am. Chem. Soc. 116 (1994) 10152–10158.
[21] T. Jirsak, J.A. Rodriguez, J. Hrbek, Surf. Sci. 426 (1999) 319–335.
[22] J.A. Rodriguez, T. Jirsak, J. Hrbek, J. Phys. Chem. B 103 (1999) 1966–1976.
[23] J.H. Lunsford, J.P. Jayne, J. Phys. Chem. 69 (1965) 2182–2184.

[24] M.J. Lin, J.H. Lunsford, J. Phys. Chem. 80 (1976) 635–639.
[25] R.A. Schoonheydt, J.H. Lunsford, J. Catal. 26 (1972) 261–271.
[26] Y. Ben Taarit, J.H. Lunsford, J. Phys. Chem. 77 (1973) 1365–1367.
[27] R.A. Schoonheydt, J.H. Lunsford, J. Phys. Chem. 76 (1972) 323–328.
[28] E.J. Karlsen, M.A. Nygren, L.G.M. Pettersson, J. Phys. Chem. B 107 (2003) 7795–7802.
[29] W.F. Schneider, J. Li, K.C. Hass, J. Phys. Chem. B 105 (2001) 6972–6979.
[30] M. Nygren, L.G.M. Pettersson, Chem. Phys. Lett. 230 (1994) 456–462.
[31] E.J. Karlsen, M.A. Nygren, L.G.M. Pettersson, J. Phys. Chem. A 106 (2002) 7868–7875.
[32] A. Snis, H. Miettinen, J. Phys. Chem. B 102 (1998) 2555–2561.
[33] M. Chiesa, M.C. Paganini, E. Giamello, D.M. Murphy, C. Di Valentin, G. Pacchioni, Acc. Chem. Res. 39 (2006) 861–867.
[34] M. Chiesa, M.C. Paganini, G. Spoto, E. Giamello, C.D. Valentin, A.D. Vitto, G. Pacchioni, J. Phys. Chem. B 109 (2005) 7314–7322.
[35] M. Chiesa, M.C. Paganini, E. Giamello, ChemPhysChem 5 (2004) 1897–1900.
[36] M. Chiesa, M.C. Paganini, E. Giamello, C. Di Valentin, G. Pacchioni, Angew. Chem. Int. Ed. 42 (2003) 1759–1761.
[37] C. Di Valentin, D. Ricci, G. Pacchioni, M. Chiesa, M.C. Paganini, E. Giamello, Surf. Sci. 521 (2002) 104–116.
[38] M. Chiesa, E. Giamello, D.M. Murphy, G. Pacchioni, M.C. Paganini, R. Soave, Z.J. Sojka, Phys. Chem. B 105 (2001) 497–505.
[39] M.C. Paganini, M. Chiesa, P. Martino, E. Giamello, J. Phys. Chem. B 106 (2002) 12531–12536.
[40] P. Meriaudeau, J.C. Vedrine, Y. Ben Taarit, C. Naccache, J. Chem. Soc., Faraday Trans. 71 (1975) 736–748.
[41] A.J. Tench, P. Holroyd, Chem. Commun. (1968) 471–473.
[42] A. Adamski, T. Spalek, Z. Sojka, Res. Chem. Intermediate 29 (2003) 793–804.
[43] M. Chiesa, M.C. Paganini, G. Spoto, E. Giamello, C. Di Valentin, G. Pacchioni, J. Phys. Chem. B 109 (2005) 7314–7322.
[44] G. Preda, G. Pacchioni, M. Chiesa, E. Giamello, J. Phys. Chem. C 112 (2008) 19568–19576.
[45] E. Giamello, D. Murphy, L. Marchese, G. Martra, A. Zecchina, J. Am. Soc., Faraday Trans. 89 (1993) 3715–3722.
[46] M. Chiesa, E. Giamello, Chem.–Eur. J. 13 (2007) 1261–1267.
[47] S. Livraghi, M.C. Paganini, M. Chiesa, E. Giamello, Res. Chem. Intermediate 32 (2006) 777–786.
[48] T. Kaljuvee, A. Trikkel, R. Kuusik, V. Bender, J. Therm. Anal. Calorim. 80 (2005) 591–597.
[49] A.L. Goodman, P. Li, C.R. Usher, V.H. Grassian, J. Phys. Chem. A 105 (2001) 6109–6120.
[50] M.C. Paganini, M. Chiesa, F. Dolci, P. Martino, E. Giamello, J. Phys. Chem. B 110 (2006) 11918–11923.
[51] M.C. Paganini, M. Chiesa, P. Martino, S. Livraghi, E. Giamello, Stud. Surf. Sci. Catal. 155 (2005) 441–449.
[52] G. Spoto, E.N. Gribov, G. Ricchiardi, A. Damin, D. Scarano, S. Bordiga, C. Lamberti, A. Zecchina, Prog. Surf. Sci. 76 (2004) 71–146.